A novel multilayer micro-ring resonator based optical network on chip

M. CHANNOUFI[a,b*], P. LECOY[b], S. LE-BEUX[c], R. ATTIA[a], B. DELACRESSONNIERE[d]
[a]*SERCOM (Laboratory of Electronic Systems and Communication Networks), Polytechnic school of Tunisia, Tunisia*
[b]*ETIS (Research Team in Information Processing and Systems), ENSEA - University of Cergy-Pontoise - CNRS, France*
[c]*Lyon Institute of Nanotechnology, Central School of Lyon, France*
[d]*LaMIPS (Laboratory of Microelectronics and Physics of Semiconductors), CRISMAT-NXPSemiconductors-PRESTO engineering, CNRS, Caen, France*

The next generation of multiprocessor systems on chip requires development and improvement of innovative implementations of optical networks on chip (ONoC). ONoC efficiency mostly relies on crosstalk between waveguides and on optical power loss. Taking into account new integration capabilities in order to achieve the best design compromise minimizing power loss and crosstalk is thus mandatory. In this paper, we propose a novel switch implementation based upon a multi-layer microring resonator, allowing efficient light coupling and switching between superposed waveguides. Such microring resonator avoids waveguide crossing, thus contributing to reduce propagation losses. A transmission loss from -4.8 to -7 dB, crosstalk between -17 and -29 dB, a quality factor about 202 allowing a bandwidth up to 1THz, are demonstrated with a 1.65 µm radius microring. Furthermore, this paper demonstrates that pure curvature loss remains less than -0.4 dB for microring radii less than 2µm thus allowing miniaturization of switch size.

(Received February 12, 2013; accepted March 13, 2014)

Keywords: Optical design and fabrication, Resonators, Multilayers

1. Introduction

With the growing need of high bandwidth and low power consumption in increasingly complex VLSI designs, communication inside the chip is becoming a bottleneck. The next generation of systems on chip will consist of heterogeneous multicore architectures where Network on Chip (NoC) will play a key role. Introduction of optical technologies makes possible to increase data throughput, decrease power consumption and miniaturize chip size. Optical Networks on Chip (ONoC) can use remarkable capabilities of photonics on silicon to create highly integrated platforms transmitting and receiving optical signals. Key elements, such as photo-detectors [1], low power driven optical modulators [2] and optical switches [3-6,14] reaching 40 Gb/s [7], have been extensively studied. Unless using optical medium, optical power losses and crosstalk seem to be an obstacle to continue progress. Using 3D multi-level waveguides can overcome such problems. In 2008, Vlasov and IBM research team [8] have estimated that integration of 3D ONoC using optical switches would begin in 2018 with 22nm CMOS technology and allow aggregate bitrates higher than 70 Tbps inside the chip. In this paper we demonstrate that insertion loss increases in vertical coupling comparing to the lateral one. For that we present a novel 2-level microring resonator merging between vertical and lateral coupling; comparison with a 1-level microring resonator demonstrates the potential of the multi-layer paradigm thus by avoiding waveguide crossing losses and decreasing crosstalk. Furthermore, comparisons with a 3-level microring resonator [9] demonstrate that physical limits such as optical coupling losses, material effects and absorption need to be carefully considered. In section 2, simulation results using Comsol software of one-level and multi-level microring resonators are presented. In section 3, insertion losses, crosstalk, bend loss, coupling coefficients, Quality factor and bandwidth are evaluated and the results are discussed.

2. Silicon photonic ring resonators design

2.1 One level silicon photonic ring resonator design

Ultra-compact microresonators enable large-scale integration and single-mode operation for a broad range of wavelengths. Such a device allows routing data from a waveguide to another according to its resonance wavelength and its state (on or off). In all the implementations proposed in this paper, the switching element consists of two crossing waveguides (channel waveguides Si (refractive index n=3.5) in SiO_2 (refractive index n=1.45)) with a width of 450 nm and a height of 300 nm and a resonant ring with a diameter of 3.3 µm. Fig. 1(a) represents an optical switch implemented on a single layer, i.e. involving waveguide crossing. In this one-level

implementation the optical switch resonates at four frequencies (Fig. 2) in the frequency window [194-212 THz] with an insertion loss of 3.5 dB and a crosstalk in the range from-10 to -17 dB. The crosstalk is defined as the part of the input power remaining in the same waveguide instead of being coupled in the second one at resonance. In any ONoC architecture, the crossing of waveguides increases insertion losses and crosstalk, involving a degradation of reception quality. The 3 implementations in this paper are studied using 3D-Comsol models. Material absorption and straight guide power loss appear higher with the 3D models, which should be more accurate because the 3D-software calculates the wave over 3D volume using the 3 planes and takes into account more radiance effects. Comsol simulations are done using RF models and FEM (Finite Element Method) solving method with PARADISO solver [18] and simulation step of 1 THz. The package PARDISO is a thread-safe, high-performance, robust, memory efficient and easy to use software for solving large sparse symmetric and unsymmetric linear systems of equations on shared-memory and distributed-memory multiprocessors.

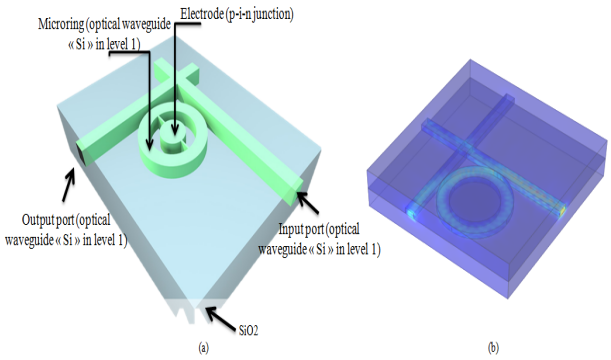

Fig. 1. (a) Schematic layout of a 1-waveguide level based microresonator. (b) Comsol simulation for a 1 waveguide level based microring resonator in ON state.

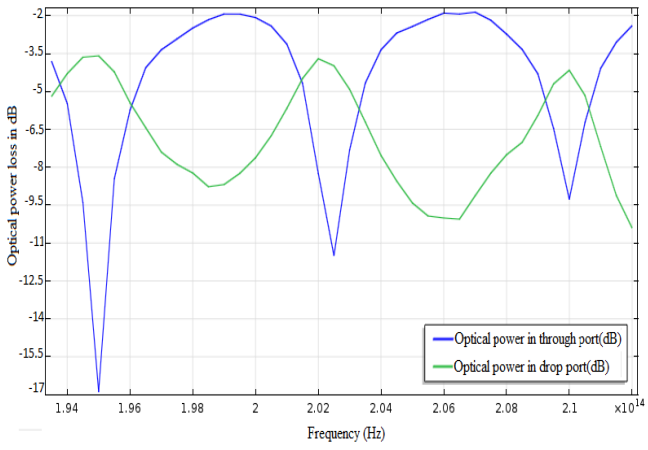

Fig. 2. Coupling (drop port) and crosstalk (through port) in dB showing different resonance frequencies for 1-level ring resonator.

In an ONoC based 3D chip the electrical (CMOS) layer sends electrical signals through specific wires in order to drive microring resonators placed in the ONoC layer. These electrical command signals are injected through short vertical metallic interconnections called TSV (Through Silicon Vias) with lengths ranging from several microns to several tens of microns (see Fig. 3). The use of a vertical p-n junction maximizes the overlap of the resonator mode with the depletion zone, enabling changes in the effective index thus in the resonance frequency, which can be achieved with low reverse voltages. This resonance shift allows optical signals either to be switched to the adjacent (drop) waveguides when ON-resonance, or to remain in the same waveguide (or direction) when OFF-resonance [11][13].

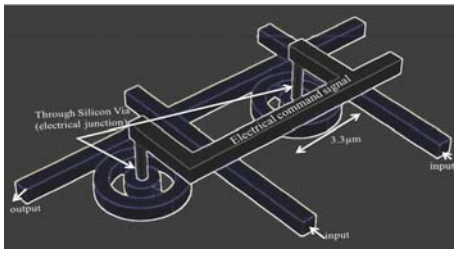

Fig..3. bottom view of the 2-level microring switch in 3D chip.

2.2 Muli-level silicon microring resonator design

Stacked waveguides are useful to minimize crosstalk and power loss in ONoCs, moreover, the efficiency of such structures depends on the feasibility of multi-level waveguides based optical switches. In this paper, two implementations relying on 2 and 3 layers are considered:

-in our proposed implementation called 2-levels switch, the ring is located under the upper waveguide and adjacent to the lower one with a gap of 100 nm between ring and waveguides, as illustrated in Fig. 4(a).

-in the second one, called 3-levels switch (Fig. 5(a)), the ring is located in a third (intermediate) layer, i.e. upper to the lower waveguide and under the higher one with a gap of 100 nm between each one. This implementation was proposed by Biberman et al [9].

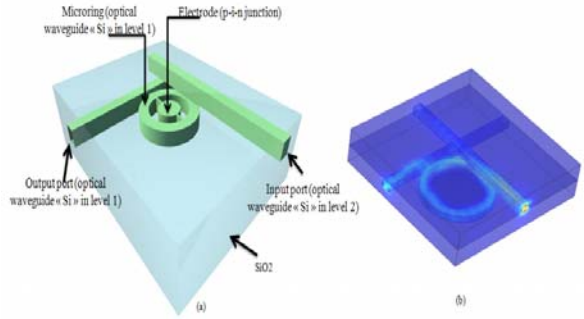

Fig. 4.(a) Schematic layout of 2 waveguide levels based microresonator. (b) Comsol simulation for 2 waveguide levels based microring resonator in ON state.

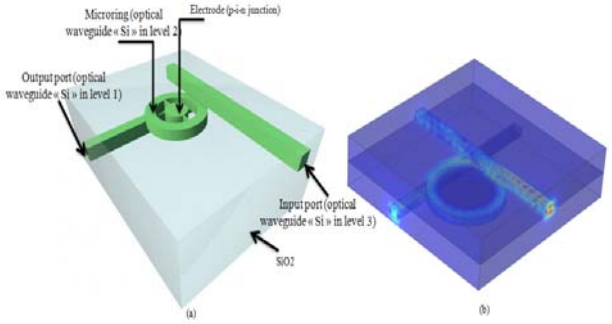

Fig. 5.(a) Schematic layout of 3 waveguide levels based microresonator. (b) Comsol simulation for 3 waveguide levels based microring resonator in ON state.

3. Simulation results and discussions

3.1 Optical power loss and Crosstalk

In the 2-level waveguide implementation the switch resonates at 195 THz, 202.5 THz and 210 THz in the frequency window [194-212 THz] with a transmission loss of -5 dB and a crosstalk varying between -17 and -22 dB (power remaining in the first guide) with a FSR (free spectral range) of 60 nm, as shown in Fig. 6 (a). In the 3-level implementation the same resonance frequencies appear and the transmission loss varies between -7 and -8 dB with a crosstalk varying between -18 and -29 dB and a FSR of 60 nm, as seen in Fig. 6 (b).

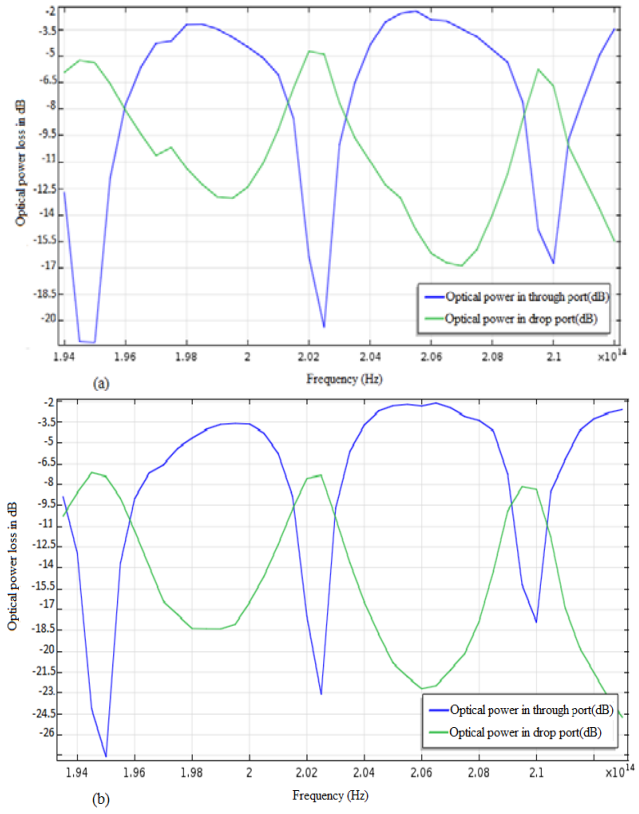

Fig. 6. Coupling (drop port) and crosstalk (through port) in dB showing for different resonance frequencies for (a) 2-level and (b) 3-level optical switch implementations.

3.2 Microresonator modeling

Coupling coefficients are then determined by the following analysis. We model wave transfer from a waveguide to another through the microresonator using crossing waveguides (as shown in Fig. 7), where the complex amplitudes of the fields, E_i,(i = 1 to 7) are represented.

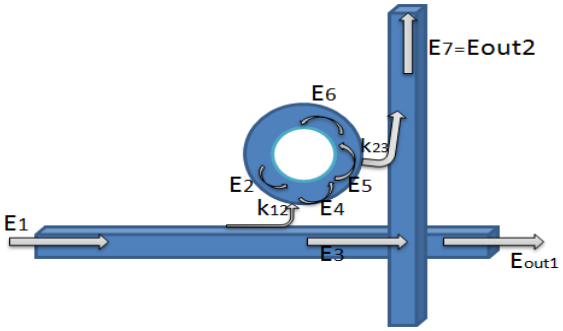

Fig. 7. Wave coupling in a microresonator with crossing waveguides.

The light transfer from the first waveguide to the ring is formalized as follow:

$$\begin{vmatrix} E_3 \\ E_4 \end{vmatrix} = \begin{vmatrix} \sqrt{1-k_{12}^2} & -jk_{12} \\ -jk_{12} & \sqrt{1-k_{12}^2} \end{vmatrix} \cdot \begin{vmatrix} E_1 \\ E_2 \end{vmatrix} \quad (1)$$

The field propagation in the ring from the first coupling point to the second one (a quarter of its circumference) is given by:

$$E_5 = E_4 . \exp\left(\frac{-(\alpha_{MR} + j\beta)L}{4}\right) \quad (2)$$

The transfer of light from the ring to the second waveguide is given by:

$$\begin{vmatrix} E_6 \\ E_7 \end{vmatrix} = \begin{vmatrix} \sqrt{1-k_{23}^2} & -jk_{23} \\ -jk_{23} & \sqrt{1-k_{23}^2} \end{vmatrix} \cdot \begin{vmatrix} E_5 \\ 0 \end{vmatrix} \quad (3)$$

The propagation from the second coupling point to the first is given by:

$$E_2 = E_6 . \exp\left(\frac{-3(\alpha_{MR} + j\beta)L}{4}\right) \quad (4)$$

Using those relations, the field coupled to the second waveguide for the microresonator geometry of Fig. 7 is given by:

$$E_{out2} = \frac{-k_{23}k_{12}\exp(-(\alpha_{MR}+j\beta)L/4)}{1-\sqrt{1-k_{12}^2}\sqrt{1-k_{23}^2}\exp(-(\alpha_{MR}+j\beta)L)}.E_1 \quad (6)$$

The insertion loss at resonance, when βL=2pπ (p is an integer) so cos(βL)=1 and sin(βL)=0, is given by:

$$IL_{res} = -20\log\left(\frac{k_{23}k_{12}\exp(-\alpha_{MR}.L/4)}{(1-\sqrt{1-k_{12}^2}\sqrt{1-k_{23}^2}\exp(-\alpha_{MR}L))}\right) \quad (7)$$

Where α_{MR} is the propagation loss in the ring waveguide (in cm^{-1}), R is the ring radius, L is its length (L = 2πR), k_{12} and k_{23} are the coupling coefficients respectively from first guide to ring, and from ring to second waveguide.

3.3 Bend radius effect

Fig. 8 shows simulation results of pure bending loss for different radii, these results are obtained by subtracting optical power loss in a straight waveguide from overall optical power loss in a half ring with the same dimensions.

Simulation results using Comsol software show that the intrinsic propagation losses in the ring with radii from 1 to 5 µm are varying from 1.4dB to 3.5dB (as shown in dashed line in Fig. 9) in the TE mode at the wavelength λ=1.42µm (non-resonant state). On the other hand, pure bend losses are varying from 0.4dB for R=1µm to less than 0.01dB for radii up to 9µm (as shown in Fig. 8). While propagation losses increase linearly with the ring radius, bend loss remains weak even with small radii. In order to optimize the design of our multi-level switches, these results demonstrate an optimal radius in the range 1.5µm to 2µm minimizing the overall microresonator insertion loss, allowing the miniaturization of the device, as shown in Fig. 9 (curve with black dashed line). Furthermore, these results justify the choice of the ring radius used in our 3 switches implementations (mono-level, 2-level and 3-level).

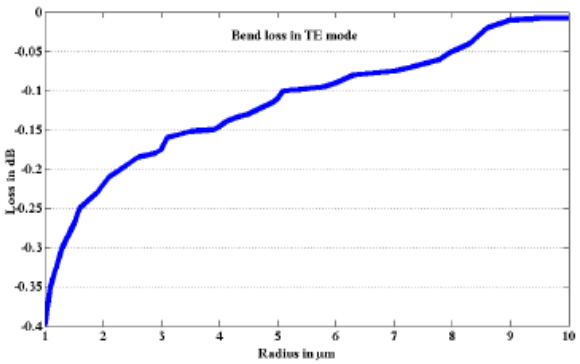

Fig. 8. Bend losses for different rings radius in TE mode.

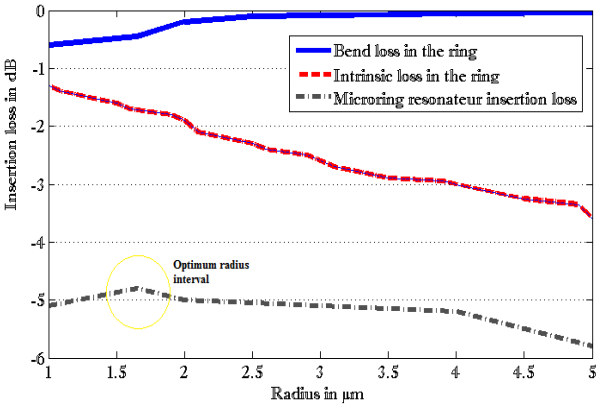

Fig. 9. Propagation ring losses for different radius in TE mode.

Table 1 shows bending losses in Si/SiO_2 waveguides measured experimentally by [15-17] for different waveguide dimensions and radii. These results demonstrate that pure bending losses are very low and don't present the primary factor of propagation losses in silicon in silica waveguides.

Table 1. Comparison of bending losses in the TE mode for Si/SiO2 waveguides.

Reference	Height (nm)	Width (nm)	Radius (µm)	Loss (dB/turn)	Wavelength (µm)
This work	300	450	1	0.4	1.42
			2	0.25	1.42
			>5	<0.01	1.42
[15]	220	445	1	0.086	1.5
			2	0.013	1.5
			5	0.005	1.5
[16]	300	300	2	0.46	1.55
			3	0.17	1.55
[17]	200	500	0.5	0.5	1.54
			0.3	0.3	1.54

In the following of this study, the ring radius is 1.65 µm for all switch implementations and we focus on insertion loss and coupling coefficient at resonance frequencies of 1.48µm and 1.53µm.

3.4 Coupling coefficient

Insertion loss for lateral and vertical coupling are studied first using Comsol software as shown in Fig. 10.

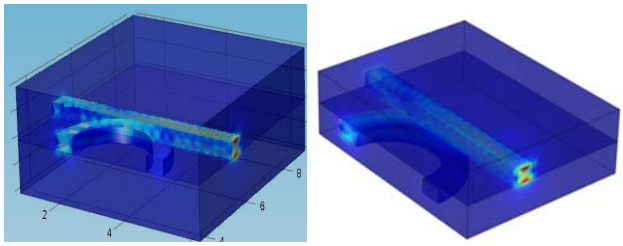

Fig. 10. (a) 3D-Comsol (FEM method) 3D-Comsol simulation for waveguide-to-ring lateral coupling for a multi-level switch. (b) 3D-Comsol simulation for waveguide-to-ring vertical coupling for a multi-level switch.

In lateral coupling between the waveguide and the ring placed in same layer, the coupling coefficient was simulated at the resonance wavelength of 1.48µm (Fig. 10(a)) and was found to be 0.81 (-0.68dB). For vertical coupling from a layer to another (Fig. 10(b)), the coupling coefficient between the waveguide and the ring placed in lower layer was found to be 0.6 (-2.15dB). Using those results, the transmission loss in a 2-level switch should be 4.83dB and 6.2dB for 3-level switch. That confirms the previous results founded by simulation of the full device for the 2-level and 3-level switch implementations (Fig. 6). Difference between coupling coefficients in lateral and vertical implementations could be explained by the scattering effects which are difficult to separate from insertion loss. From these results, we assume that scattering loss is more important in vertical coupling as the light coupling area is wider (coupling in 2 planes) than in lateral coupling where light coupling occures in the same plane.

As identical microring dimensions and waveguide material parameters are used in the three implementations, bend losses and material effect values should be the same. By comparing the simulation results, we observe that by adding layers the transmission loss increases while the crosstalk is decreases. The purpose of this study is to find a compromise from these results in order to optimize communication within the network-on-chip architecture, ensuring a low crosstalk with reasonable transmission loss.

3.5 Quality factor and bandwidth

The microring is expected to have a much wider bandwidth than the bandwidth required by the ONoC data rate, in order not to limit it. Basically, the bandwidth of a microring is driven by the modulation speed which depends on the optical lifetime (extinction ratio) of the microring resonators. The quality factor Q gives an estimation of the number of optical cycles that will last confined within a resonator. It is usually defined as the ratio of the energy stored to the energy dissipated in the microresonator. The quality factor Q of the ring at resonance is given by [12]:

$$Q_{res} = \frac{4\pi^2 Rn_{eff}}{\lambda_0 (1 - \chi_r^2)} \quad (8)$$

Where $\chi_r = \exp(-2\pi R\alpha_{MR})$ is the round trip amplitude loss factor, λ_0 is the resonance wavelength taken at 1.48 µm (corresponding to the resonance frequency of 202.5 THz), n_{eff}= 3.07 is the effective index, and R is the microring radius (1.65µm).

Using these parameters and eq (8) the quality factor is found to be 202 for a micro-ring resonator with a 1.65 µm radius, and an intrinsic loss of 2.45 dB. The high Q-factor of the microring resonator involves a narrow resonance linewidth, long switching time, and high optical intensity, while lower Q-factor microrings allow higher bandwidths. The optical bandwidth of the resonator, defined as the full width at half maximum (FWHM) and computed as ν/Q where ν is the resonance frequency and Q is the quality factor, is then near 1 THz. Those results show that the micro-ring switches have an optical bandwidth much greater than the bandwidth of transmitters and will not be an obstacle to the growth of throughputs (achieving until now 40 Gbps with a BER of 10^{-9} [7]). The main advantage of the multi-level switches is to reduce crosstalk, improving reception quality.

3.6 Discussion

ONoCs are usually composed of hundreds or even thousands of crossing waveguides and optical switches. Using multi-level waveguide based switches prevents losses caused by crossing waveguides and allows an increase of the number of processor cores connected in one chip while keeping the same number of waveguides and switches. Hence, careful selection of switch implementation is mandatory since cumulative effect of propagation losses will occur. Design tradeoff thus needs to be achieved based on simulation results. As seen in Table 2, by increasing the number of layers, the propagation loss increases and the crosstalk decreases, and by keeping the same ring radius, bandwidth and quality factor are the same for the 3 implementations.

Table 2. Multi and single- level switch characteristics.

	1 level switch	**2 level switch**	**3 level switch**
Insertion loss from guide to guide (-dB) (respectively at 1.48µm and1.53µm)	3.5-3.8	4.8-5.3	6.8-7.2
Total loss inside the ring (-dB) (respectively at 1.48 and 1.53µm)	1.9-2.45	1.9-2.45	1.9-2.45
Material loss inside the ring (-dB)	1.75-2.2	1.75-2.2	1.75-2.2
Crosstalk(-dB)	10-17	17-23	18-29
Q_{int} (at 1.48µm)	202	202	202
Bandwidth(THz)	1	1	1

However, the main trend in the design of ONoCs is to reduce the power consumption for scalability purpose. In such a scenario, using the proposed 2-level switch implementation is more suitable because it will contribute to reduce the ONoC power consumption, at the cost of a higher, but still acceptable, crosstalk compared to 3-level implementation. Power reduction can indeed be achieved by reducing laser output power, which is made possible by the reduction of propagation losses in the optical paths. Another economical reason for using the 2-level implementation instead of the 3-level one is its lower design and processing cost.

4. Conclusion

Two implementations of multi-level coupled silicon microring electrooptic switch of 3.3 μm diameter were characterized. Insertion losses in the range of 4.8 to 7 dB and crosstalk in the range of -17 to -29 dB were found by FEM-method. This could lead to improve the performance of optical networks on chip by minimizing the optical power loss and crosstalk between processors. A Quality factor in the range of 202 allowing an optical bandwidth higher than 1 THz was found. In ONoCs, the optical power budget represents the energy required to propagate a signal from a laser source to a photodetector; it depends on losses occurring in passive optical devices where the optical signals travel. Hence, multi-level microring resonator contributes to reduce the optical power budget without affecting the reception quality. Such improvement leads to new opportunities to ONoC designers: energy can be saved to achieve optical communication and the ONoC size can be increased to interconnect additional resources (e.g. processors and memories).

References

[1] L. Chen, P. Dong, M. Lipson Optics Express, **16**(15), 11513 (2008).
[2] William M. Green, Michael J. Rooks, Lidija Sekaric, Yurii A. Vlasov, Optics Express, **15**(25), 17106 (2007).
[3] F. Xia, M. J. Rooks, L. Sekaric, Y. A. Vlasov, Optics Express, **15**(19), 11934 (2007).
[4] Xi Xiao, Hao Xu, Xianyao Li, Yingtao Hu, Kang Xiong, Zhiyong Li, Tao Chu, Yude Yu, Jinzhong Yu, OSA Optics Express, **20**(3), 2507 (2012).
[5] F. Y. Gardes, A. Brimont, P. Sanchis, G. Rasigade, D. Marris-Morini, L. O'Faolain, F. Dong, J. M. Fedeli, P. Dumon, L. Vivien, T. F. Krauss, G. T. Reed, J. Martí, Optics Express, **17**(24), 21986 (2009).
[6] H. Chen, journal of optical communication, (27), 208 (2006).
[7] L. Xu, W. Zhang, Q. Li, J. Chan, H. L. R. Lira, M. Lipson, K. Bergman, IEEE Photonics Technology Letters, **24**(6), 473 (2011).
[8] Yuri Vlasov "Silicon photonics for next generation computing systems" ECOC 2008.
[9] A. Biberman, K. Preston, G. Hendry, N. Sherwood-Droz, J. Chan, J. S. Levy, M. Lipson, K. Bergman, ACM Journal on Emerging Technologies in Computing Systems, **l7**(2), (2011).
[10] E. J. Klein, PhD Thesis, University of Twente, ISBN 978-90-365-2495-7, 2007.
[11] M. R. Watts, W. A. Zortman, D. C. Trotter, R. W. Young, A. L. Lentine, Opt. Express, **19**(22), 21989 (2011).
[12] W. D. Sacher, J. K. S. Poon, J. Lightwave Technol. **27**(17), 3800 (2009).
[13] H. L. R. Lira, S. Manipatruni, M. Lipson, Opt. Express **17**(25), 22271 (2009).
[14] C. K. Madsen, J. H. Zhao, John Wiley & Sons (ISBN: 0-471-18373-3), May 1999.
[15] Y. A. Vlasov, S. J. McNab, Opt. Express, **12**(8), 1622 (2004).
[16] T. Tsuchizawa, E. Watanabe, Tamechika, T. Shoji, K. Yamada, J. Takahashi, S. Uchiyama, S. Itabashi, H. Morita, Paper TuU2 presented at LEOS Annual Meeting, p.287, Glasgow, UK (2002).
[17] D. R. Lim, "Device integration for silicon microphotonics platforms," PhD thesis, MIT (2000).
[18] http://www.pardiso-project.org/

*Corresponding author: malek.channoufi@ensea.fr